Korean Journal of Remote Sensing, Vol.27, No.3, 2011, pp.289~301

Sub-class Clustering of Land Cover over Asia considering 9-year NDVI and Climate Data

Ga-Lam Lee*, Kyung-Soo Han †, and Do-Yong Kim*****

*Geoinformatic Engineering Research Institute, Pukyong National University, Busan, Korea

**Department of Spatial Information Engineering, Pukyong National University, Busan, Korea

***BK21 Graduate School of Earth Environmental System, Pukyong National University, Busan, Korea

Abstract : In this paper an attempt has been made to classify Asia land cover considering climatic and vegetative characteristics. The sub-class clustering based on the 13 MODIS land cover classes (except water) over Asia was performed with the climate map and the NDVI derived from SPOT 5 VGT D10 data. The unsupervised classification for the sub-class clustering was performed in each land cover class, and total 74 clusters were determined over the study area. Via these clusters, the annual variations (from 1999 to 2007) of precipitation rate and temperature were analyzed as an example by a simple linear regression model. The various annual variations (negative or positive pattern) were represented for each cluster because of the various climate zones and NDVI annual cycles. Therefore, the detailed land cover map as the classification result by the sub-class clustering in this study can be useful information in modelling works for requiring the detailed climatic and vegetative information as a boundary condition.

Key Words : land cover, sub-class clustering, climate map, NDVI, SPOT VGT

1. Introduction

Land cover plays an important in many Earth system process due to the interaction between the Earth's surface and the atmosphere. Land cover information is a critical parameter in hydrological models (Sandholt *et al.*, 1999; Droogers and Kite, 2002; Yang and Musiake, 2003), biophysical models (Kimball *et al.*, 1999; Liu *et al.*, 2002; Lotsch *et al.*, 2003; Inoue and Olioso, 2004), and climatological models (Champeaux *et al.*, 2000; Chase *et al.*, 2000). Recent works in classifying regional, continental and global land cover have seen the application of multi-temporal remotely sensed data sets, which describe vegetation dynamics by viewing their phenological variation throughout the course of a year (Verhoef *et al.*, 1996). Tucker *et al.* (1985), Townshend *et al.* (1987), and Stone *et al.* (1994) have produced continental-scale classifications of land cover using this approach. For global land cover products, DeFries and Townshend (1994b) derived a one-by-one degree map and more recently an 8 km map

Received May 27, 2011; Revised June 14, 2011; Accepted June 15, 2011.

† Corresponding Author: Kyung-Soo Han (kyung-soo.han@pknu.ac.kr)

(DeFries *et al.*, 1998) using the Advanced Very High Resolution Radiometer (AVHRR) data. The current global land cover products are much finer in resolution than traditional climate modelers require, although there are some who have begun to take advantage of the additional information in the depiction of landscape heterogeneity provided by finer resolutions (Dickinson, 1995; Hansen *et al.*, 2000).

Use of remotely sensed data from satellite makes susceptible to various interpretations and extraction of thematic information, such as land cover and use, about Earth's surface at multiple spatial scales (Park *et al.*, 2006). Maps produced using satellite data have advantages over traditional ground based maps due to the continuous coverage and internal consistency of remotely sensed data sets (Hansen *et al.*, 2000). A primary reason for attempting to create maps from these data sets is the potential for creating more accurate products, where the areas of disagreement between products are less than past efforts compiled from ground-based maps (DeFries and Townshend, 1994a; Hansen *et al.*, 2000). Satellite image estimates of vegetation cover provide important and timely information for modeling biochemical cycle and climate, carbon accounting, and monitoring ecosystem condition (Hansen *et al.*, 2002; Jang, 2006; Kim *et al.*, 2007; Lee *et al.*, 2009). Most land cover mapping applications at broad spatial scales have been based on multi-temporal Normalized Difference Vegetation Index (NDVI) data (Tucker *et al.*, 1985; Loveland *et al.*, 1991). Continental and global land cover classification from satellite data have largely been derived from annual time series of the NDVI as a measure of phenology variety throughout the year (Tucker *et al.*, 1985; Townshend *et al.*, 1987; Loveland *et al.*, 1991; Stone *et al.*, 1994; DeFries and Townshend, 1995; DeFries *et al.*, 1998). During the past 15 years, substantial progress has been made in using SPOT VEGETATION (VGT) data for land cover characterization. For example, unsupervised classification (Bartalev *et al.*, 2003; Han *et al.*, 2004; Huang and Siegert, 2006; Vancutsem *et al.*, 2009), supervised classification (Pasqualini *et al.*, 2005), a mixed approach (Latifovic and Olthof, 2004; Stibig *et al.*, 2007), tree approach (Stroppiana *et al.*, 2003; DeFries *et al.*, 1998), logical classification systems (Stibig *et al.*, 2004).

Changes in land cover due to natural and anthropogenic processes can affect the biophysical characteristics of the surface with implications for biogeochemical cycle and the energy budget (Clark *et al.*, 2001; Bounoua *et al.*, 2002; Fuller and Ottke, 2002; Cabral *et al.*, 2003, 2006). Also, there may be various vegetative and climatic conditions in a land cover class. Therefore, it is necessary to consider vegetation and climate changes for the classifying land cover. Champeaux *et al.* (2004) described the methods used to derive surface parameters at 1km resolution using land cover maps, climate maps, and NDVI datasets. They introduced a new concept of re-classification on a land cover type to identify heterogeneity intra land cover class over Africa and Europe. The study attempted this concept (hereafter, so-called sub-class clustering) over Asia continent. In this study, Sub-class clustering of Asia land cover was performed with SPOT VGT data and climate map, based on the MODerate resolution Imaging Spectroradiometer (MODIS) global land cover map. Via the detailed land cover map as the classification result by sub-class clustering, the annual variations of precipitation rate and temperature were analyzed.

2. Study area and data

The study area encompasses 24 countries in Asia, ranging from 68° E to 180° E and from 55° N to -12° N (Fig. 1). Study area contains a variety of climate

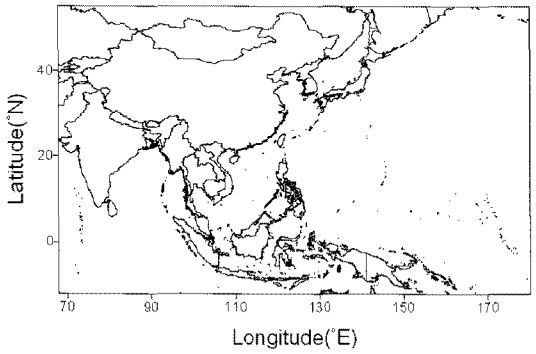

Fig. 1. Location of study area over Asia, ranging from 68° E to 180° E and from 55° N to -12° N.

zone, including tropical and subtropical in south area, littoral in southern islands, polar and sub polar in northern continental region. Northern Asia has much the same sort of climate as central Asia, except that is has more rainfall. Winters are extremely cold-the coldest inhabited place in the world is a village in Siberia. Southern Asia is hot all year around and there is a rainy season and a dry season. Eastern Asian is influenced monsoon.

Many kinds of global land cover are currently available, UMD(University of Maryland) 1 km global land cover maps, International Geosphere-Biosphere Programme, Data and Information Systems(IGBP-DIS) land cover, Global Land Cover(GLC) 2000, MODIS global land cover. These global land cover data sets were created for the same fundamental purpose of providing improved global land cover information for environmental modelers. The MODIS land cover map produced by Boston University at approximately 1km spatial resolution (Friedl *et al.*, 2002) was used in this study, and shown in Fig. 2 for the study area. The study area contains 14 land cover classes (water, evergreen needleleaf forest, evergreen broadleaf forest, deciduous needleleaf forest, deciduous broadleaf forest, mixed forests, closed shrublands, open shrublands, woody savannas, savannas, grasslands, croplands, urban and built-up, barren or sparsely vegetated).

The climate map developed by Koeppe and De Long (1958) was used in this study to decide the number of sub-class cluster in each MODIS land cover class. The study area contains 16 climate zones (tropical desert, wet and dry tropical, trade wind littoral, semiarid continental, cool marine, humid continental, cold with dry winter, wet equatorial, semiarid tropical, warm littoral, humid subtropical, international desert, polar, extreme subpolar, cold littoral, warm with dry winter).

NDVI derived from SPOT 5 VGT D10 data (Duchemin and Maisongrande, 2002; Hagolle *et al.*, 2004) during 2008 was used in this study. The Earth observation satellite SPOT 5 with VGT 2 instrument onboard was launched on MAY 4th, 2002. The VGT 2 instrument has two types product. One is P-product and the other is S-product. The instrument provides spectral reflectance measurements, which are delivered to users in the form of four standard products as follows:

(a) P product: physical values of spectral reflectance on the top-of-atmosphere;

(b) S1 product: daily maximum of NDVI composite of spectral reflectance at the top of-canopy;

(c) S10 product: ten-day maximum of NDVI composite of spectral reflectance at the top-of-canopy;

(d) D10 product: ten-day composite of directionally normalized spectral reflectance at the top-of-canopy.

The NCEP/NCAR reanalysis (Kalnay *et al.*, 1996; Kistler *et al.*, 2001) provides long-term model analysis ideal for the study and initialization of global- and regional-climate-scale models. Global reanalysis estimates were generated using a single, 'frozen' version of an operational numerical model, which was then run for the period from 1948 to present. All reanalysis values used in this study were analyzed on a 192×94 point Gaussian grid (approximate $1.905° \text{ N} \times 1.875° \text{ E}$ resolution). The

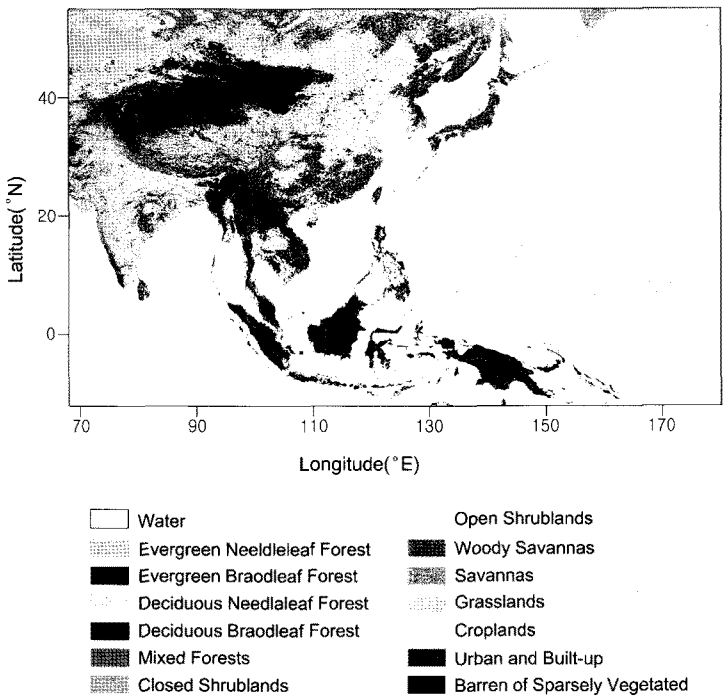

Fig. 2. MODIS land cover map of the study area contains 14 land cover classes such as water, evergreen needleleaf forest, evergreen broadleaf forest, deciduous needleleaf forest, deciduous broadleaf forest, mixed forests, closed shrublands, open shrublands, woody savannas, savannas, grasslands, croplands, urban and built-up, barren or sparsely vegetated.

monthly temperature and daily precipitation rate of NCEP/NCAR reanalysis data during 1999~2007 is used in this study.

The sub-class clustering of Asia land cover was performed by considering climate and vegetation. For determining the initial cluster, the number of climate zone in each MODIS land cover class was detected over the study area, using the climate map. The 64 initial clusters in 13 MODIS land cover classes (except water) over the study area were determined in this study. And then, the sub-class clustering by using the Iterative Self-organizing Data Analysis (ISODATA) unsupervised method (Tou and Gonzalez, 1974) was performed with the VGT D10 NDVI data in each MODIS land cover class. The ISODATA procedure is one of the widely unsupervised clustering algorithms, and commonly used for satellite image classification (Irvin *et al.*, 1997). Spectral reflectances from multiple wavebands (equivalent to attributes) are used to determine cluster in multidimensional attribute space. ISODATA technique method of unsupervised classification uses a maximum-likelihood decision rule to calculate class means that are evenly distributed in the data space and then iteratively clusters the remaining pixels, using minimum distance techniques (Melesse and Jordan, 2002). An unsupervised classification procedure was used for image classification (ERDARS version 8.6), as it allows for the identification of all the important spectral groupings without initially knowing which are the thematically significant (Cihlar *et al.*, 1998; Boles *et al.*, 2004).

3. Results and discussion

The final number of clusters by the sub-class clustering is 74, and shown in Fig. 3. The forest

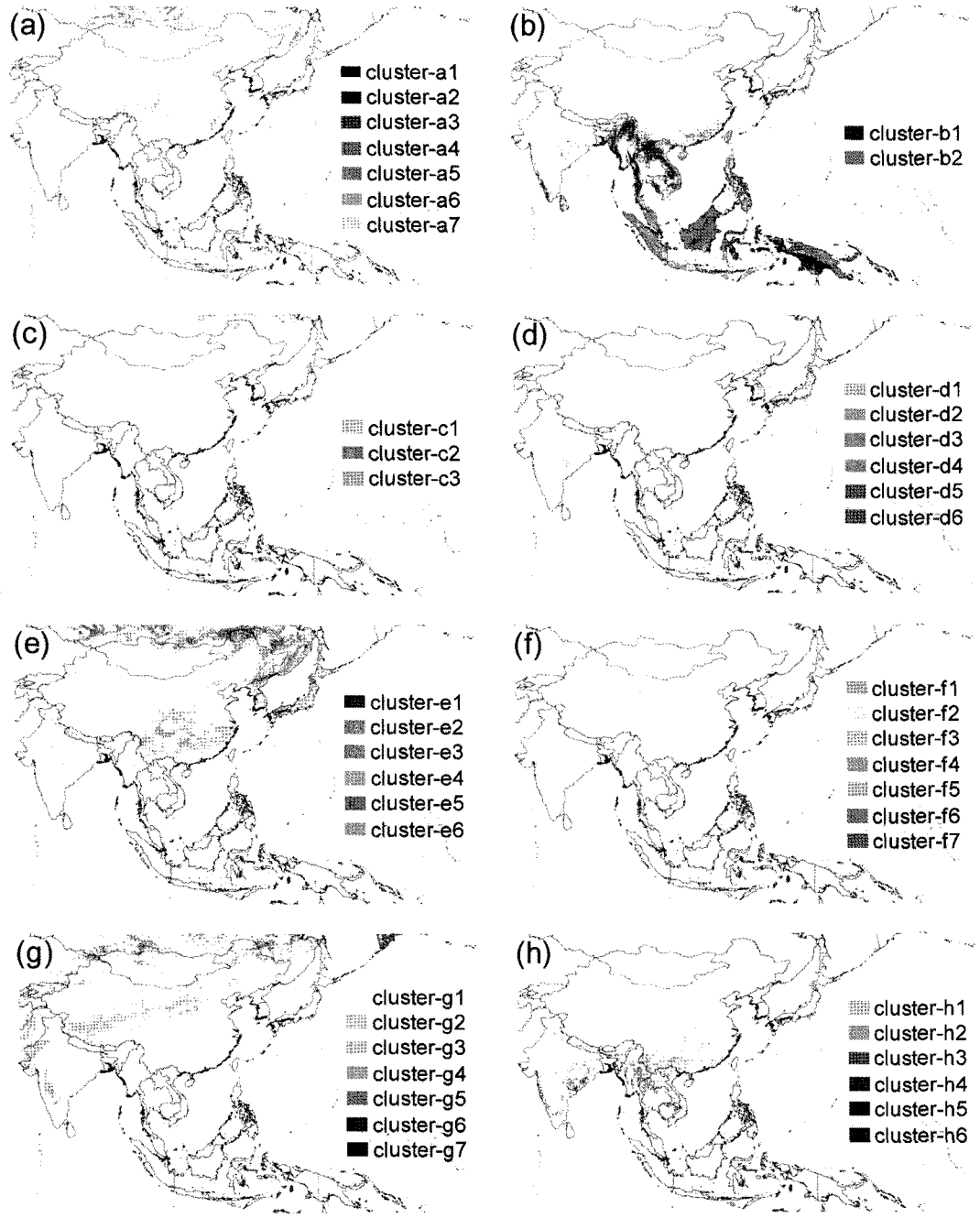

Fig. 3. The results of sub-class clustering for each MODIS land cover class, (a) evergreen needleleaf forest, (b) evergreen broadleaf forest, (c) deciduous needleleaf forest, (d) deciduous broadleaf forest, (e) mixed forests, (f) closed shrublands, (g) open shrublands, (h) woody savannas, (i) savannas, (j) grasslands, (k) croplands, (l) urban and built-up, (m) barren or sparsely vegetated.

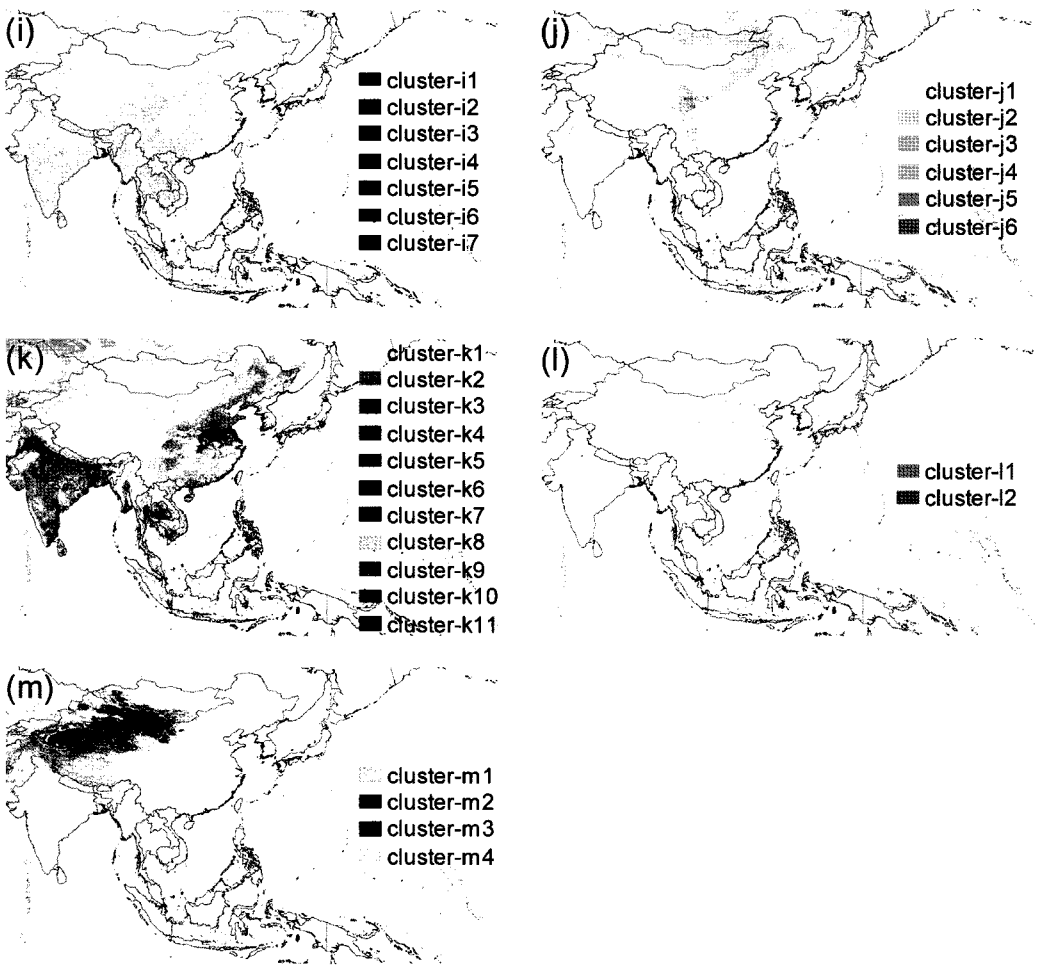

Fig. 3. Continued.

classes for evergreen needleleaf, evergreen broadleaf, deciduous needleleaf, and deciduous broadleaf were classified into 7, 2, 3, and 6 clusters, respectively (Figs. 3a, 3b, 3c, and 3d). The mixed forests class shown in Fig. 3e has 6 clusters. For the closed shrulands, open shrulands, woody savannas, and savannas classes, the number of clusters is 7, 7, 6, and 7, respectively (Figs. 3f, 3g, 3h, and 3i). The grasslands and croplands classes were classified into 6 and 11 clusters, respectively (Figs. 3j and 3k). The urban and built-up class shown in Fig. 3l has 2 clusters. For the barren or sparsely vegetated class, 4 clusters were classified (Fig. 3m). These results show heterogeneity within each land cover class. Because the climate zone and NDVI annual cycle is various for each cluster although they are in the same land cover class. Fig. 4(a) and (b) shows NDVI cycle of each cluster which is included in open shrublands class and grasslands, respectively. Every cluster has different NDVI cycle and, especially, cluster-g6 and cluster-g7 shows growth cycle different with other clusters which show little change of NDVI value. It presents heterogeneity of NDVI within the same land cover class. Table 1 shows that the percentage of

Table 1. The percentage of climatic type which is the largest portion in cluster-b1 and cluster-b2

	Cluster-b1	cluster-b2
climatic type	Wet and dry tropical	Warm littoral
percentage (%)	57	72

Table 2. Slope range of each level for annual mean precipitation rate and temperature during 1999-2007 in the study area.

	Slope range for precipitation rate(mm/h)	Slope range for temperature(℃)
Level-2	below -0.006	below -0.188
Level-1	-0.006 ~ -0.0013	-0.188 ~ -0.056
Level 0	-0.0013 ~ 0.0013	-0.056 ~ 0.056
Level+1	0.0013 ~ 0.006	0.056 ~ 0.188
Level+2	over 0.006	over 0.188

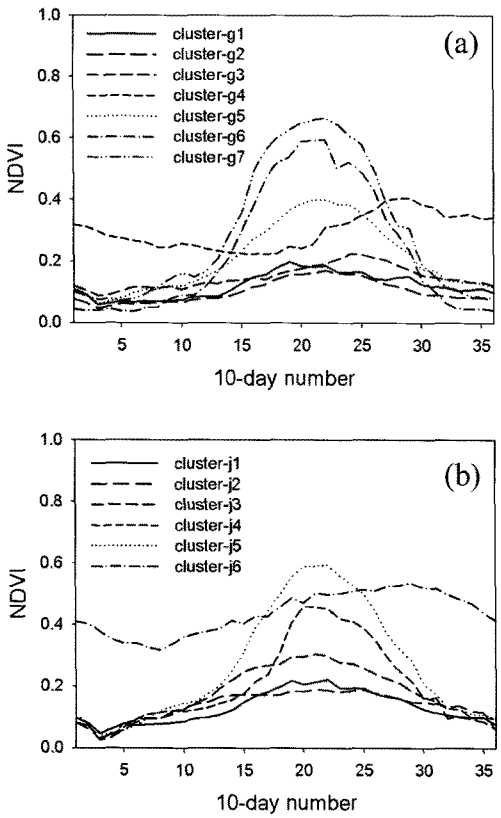

Fig. 4. The variation of NDVI in each cluster in 2008; (a) open shrublands, (b) Grasslands

climatic type which is the largest portion in cluster-b1 and cluster-b2. As a result of unsupervised classification, the clusters presented different remarkable climatic type. It means that the classification was influenced on climatic type.

The annual variations (from 1999 to 2007) of precipitation rate and temperature as the meteorological and climatological factors for the clusters classified by the sub-class clustering in this study were analyzed by a simple linear regression model. The slope as the regression coefficient of each pixel was calculated by annual mean values, and divided into 5 levels such as Level-2, Level-1, Level 0, Level+1, and Level+2. The levels were was decided by histogram using slope of the simple linear regression expression. The slope range of each level for the precipitation rate and temperature is shown in Table 2. The minus and plus signs in each slope level represent negative and positive annual variations, respectively. For example, the Level+2 for the precipitation rate means the increasing (positive) pattern over 0.006mm/h every year during the study period. For the precipitation rate, the spatial rates of each slope level for (a) cluster-b1 and (b) cluster-b2 in evergreen broadleaf forest class shown in Fig. 3b were analyzed as an example (Fig. 5). The spatial rates of Level-2 and Level-1 in cluster-b1 are 49.79% and 14.46%, respectively (Fig. 5a). It means that the negative pattern area for the annual variation of precipitation rate is wider than the positive pattern area in cluster-b1. In cluster-b2, the similar spatial rate was represented both the negative and positive

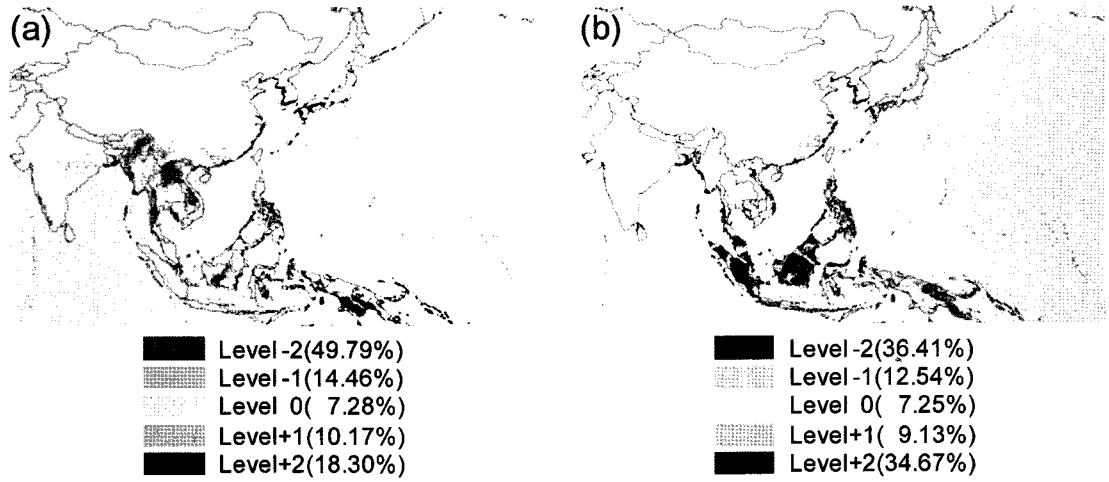

Fig. 5. The spatial rates of each slope level of annual mean precipitation rate during 1999-2007 for (a) cluster-b1 and (b) cluster-b2 in evergreen broadleaf forest class shown in Fig. 3b. The slope range of each level was represented in Table 1.

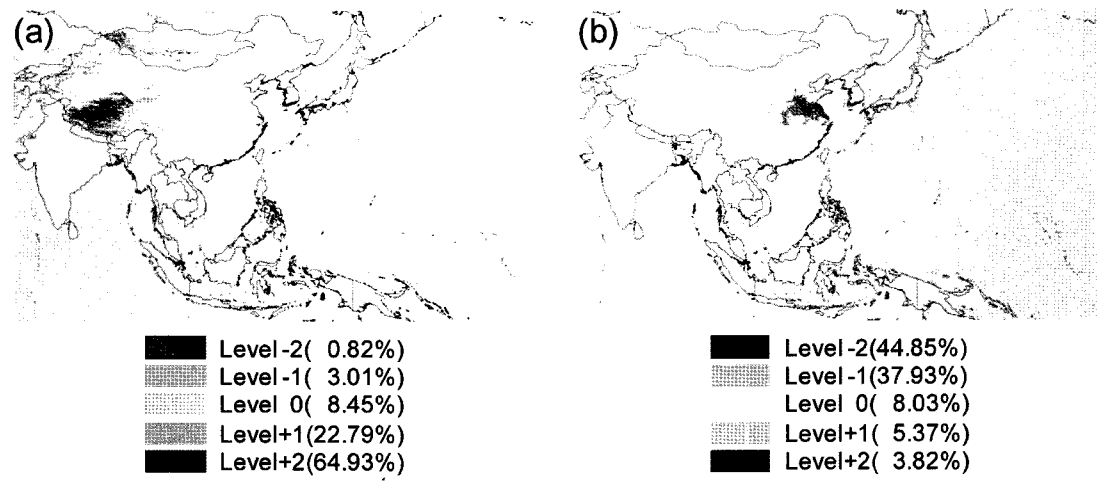

Fig. 6. The spatial rates of each slope level of annual mean temperature during 1999-2007 for (a) cluster-g2 in open shrublands class and (b) cluster-k5 in croplands class shown in Figs. 3g and 3k. The slope range of each level was represented in Table 1.

levels (Fig. 5b). The spatial rates of Level-2 and Level+2 in cluster-b2, are 36.41% and 34.67%, and represented over the large part of Sumatra Island and the southwest of Borneo Island in Indonesia, respectively. For the temperature, the spatial rates of each slope level for (a) cluster-g2 in open shrublands class and (b) cluster-k5 in croplands class shown in Figs. 3g and 3k were analyzed as an example (Fig. 6). The large part of cluster-g2 is located around Taklamakan desert, and the positive pattern area is occupied more than 85% (Level+2, 64.93% and Level+1, 22.79%) (Fig. 6a). It means that the annual variation of temperature in cluster-g2 area increases during the study period, and consistent with the Intergovernmental Panel on Climate Change (IPCC) 4th report (IPCC, 2007). Many clusters represent an increase in the annual variation of temperature, but cluster-k5 in croplands class represents the negative pattern. The spatial rates of Level-2 and Level-1 in cluster-k5 are 44.85% and 37.93%, respectively (Fig.

6b). As a whole, the various annual variations of the precipitation rate and temperature for each cluster were represented in the same land cover class. Moreover, the various spatial rates of negative and positive pattern were represented in a cluster.

4. Summary and conclusion

In this study, the sub-class clustering based on MODIS land cover was performed to develop the detailed land cover map over Asia considering climate zone and vegetation. The ISODATA unsupervised method was used for the sub-class clustering. The 64 initial clusters in 13 MODIS land cover classes (except water) over the study area were determined by the climate map. And then, the sub-class clustering was performed with the NDVI derived from SPOT 5 VGT D10 data in each MODIS land cover class, and 74 clusters were determined as follows:

(a) Evergreen needleleaf forest class : 7 clusters
(b) Evergreen broadleaf forest class : 2 clusters
(c) Deciduous needleleaf forest class : 3 clusters
(d) Deciduous broadleaf forest class : 6 clusters
(e) mixed forests class : 6 clusters
(f) Closed shrublands : 7 clusters
(g) Open shrublands : 7 clusters
(h) Woody savannas : 6 clusters
(i) Savannas : 7 clusters
(j) Grasslands : 6 clusters
(k) Croplands : 11 clusters
(l) Urban and built-up : 2 clusters
(m) Barren or sparsely vegetated : 4 clusters

The annual variations of precipitation rate and temperature were analyzed by the simple linear regression model, using NCEP/NCAR reanalysis data during 1999~2007, via the detailed land cover map as the classification result by the sub-class clustering in this study. The results were discussed with the regression slopes as the annual variation patterns for some cluster as an example. Some cluster represented the positive pattern (increasing trend) of the annual variation for each factor. There were also the negative pattern (decreasing trend) clusters. Moreover, the spatial rates of negative and positive pattern were various in a cluster. Therefore, the various variation patterns of the meteorological and climatological factors in high-resolution studies can be investigated by using the land cover classification by the sub-class clustering considering climate and vegetation. And, the results of the sub-class clustering can be useful information in modelling works for requiring the detailed climatic and vegetative information as a boundary condition. Moreover, the result of sub-class clustering does not need to analyze biophysically but it may also need to be analyzed.

Acknowledgements

This subject is supported by Ministry of Environment as "The Eco-technopia 21 project"(121 - 091 - 069).

References

Bartalev, S. A., A. S. Belward, D. V. Erchov, and A. S. Isaev, 2003. A new SPOT4-VEGETATION derived land cover map of Northern Eurasia, *International Journal of Remote Sensing*, 24(9): 1977-1982.

Boles, S., X. Xiao, J. Liu, Q. Zhang, S. Munkhtuya, S. Chen, and D. Ojima, 2004. Land cover characterization of Temperate East Asia using multi-temporal VEGETATION sensor data, *Remote Sensing of Environment*, 90(4): 477-

489.

Bounoua, L., R. DeFries, G. J. Collatz, P. Sellers, and H. Khan, 2002. Effects of land cover conversion on surface climate, *Climatic Change*, 52(1-2): 29-64.

Cabral, A. I. R., M. J. P. De Vasconcelos, J. M. C. Pereira, É. Bartholomé, and P. Mayaux, 2003. Multi-temporal compositing approaches for SPOT-4 VEGETATION, *International Journal of Remote Sensing*, 24(16): 3343-3350.

Cabral, A. I. R., M. J. P. Vasconcelos, J. M. C. Pereira, E. Martins, and É. Bartholomé, 2006. A land cover map of southern hemisphere Africa based on SPOT-4 Vegetation data, *International Journal of Remote Sensing*, 27(6): 1053-1074.

Champeaux, J. L., D. Arcos, E. Bazile, D. Giard, J. P. Goutorbe, F. Habets, J. Noilhan, and J. L. Roujean, 2000. AVHRR-derived vegetation mapping over Western Europe for use in Numerical Weather Prediction models, *International Journal of Remote Sensing*, 21 (6-7): 1183-1199.

Champeaux, J. L., K. S. Han, and V. Masson, 2004. ECOCLIMAP II: A future Global Surface Parameters Database using SPOT/VEGETATION data and the GLC2000 product, *2nd VEGETATION International Users Conference*, 2046-2049

Chase, T. N., R. A. Pielke Sr., T. G. F. Kittel, R. R. Nemani, and S. W. Running, 2000. Simulated impacts of historical land cover changes on global climate in northern winter, *Climate Dynamics*, 16(2-3): 93-105.

Cihlar, J., Q. Xiao, J. Chen, J. Beaubien, K. Fung, and R. Latifovic, 1998. Classification by progressive generalization: a new automated methodology for remote sensing multichannel data, *International Journal of Remote Sensing*, 19(14): 2685-2704.

Clark, D. B., Y. Xue, R. J. Harding, and P. J. Valdes, 2001. Modeling the impact of land surface degradation on the climate of tropical North Africa, *Journal of Climate*, 14(8): 1809-1822.

DeFries, R. S., and J. R. G. Townshend, 1994a. Global land cover: comparison of ground-based data sets to classifications with AVHRR data, In Environmental Remote Sensing from Regional to Global Scales, edited by G. Foody and P. Curran (Chichester: Wiley).

DeFries, R. S., and J. R. G. Townshend, 1994b. NDVI-derived land cover classifications at a global scale, *International Journal of Remote Sensing*, 15(17): 3567-3586.

DeFries, R. S., M. Hansen, and J. R. G. Townshend, 1995. Global discrimination of land cover types from metrics derived from AVHRR pathfinder data, *Remote Sensing of Environment*, 54(3): 209-222.

DeFries, R. S., M. Hansen, J. R. G. Townshend, and R. Sohlberg, 1998. Global land cover classifications at 8 km spatial resolution: the use of training data derived from Landsat imagery in decision tree classifiers, *International Journal of Remote Sensing*, 19(16): 3141-3168.

Dickinson, R. E., 1995. Land processes in climate models, *Remote Sensing of Environment*, 51(1): 27-38.

Droogers, P., and G. Kite, 2002. Remotely sensed data used for modelling at different hydrological scales, *Hydrological Processes*, 16(8): 1543-1556.

Duchemin, B., and P. Maisongrande, 2002. Normalisation of directional effects in 10-day global syntheses derived from VEGETATION/ SPOT: I. Investigation of concepts based on simulation, *Remote Sensing of Environment*, 81(1): 90-100.

Friedl, M. A., D. K. McIver, J. C. F. Hodges, X. Y.

Zhang, D. Muchoney, A. H. Strahler, C. E. Woodcock, S. Gopal, A. Schneider, A. Cooper, A. Baccini, F. Gao, and C. Schaaf, 2002. Global land cover mapping from MODIS: algorithms and early results, *Remote Sensing of Environment*, 83(1-2): 287-302.

Fuller, D. O., and C. Ottke, 2002. Land cover, rainfall and land-surface albedo in West Africa, *Climatic Change*, 54(1-2): 181-204.

Hagolle, O., A. Lobo, P. Maisongrande, F. Cabot, B. Duchemin, and A. De Pereyra, 2004. Quality assessment and improvement of temporally composited products of remotely sensed imagery by combination of VEGETATION 1 and 2 images, *Remote Sensing of Environment*, 94(2): 172-186.

Han, K. S., J. L. Champeaux, and J. L. Roujean, 2004. A land cover classification product over France at 1 km resolution using SPOT4/ VEGETATION data, *Remote Sensing of Environment*, 92(1): 52-66.

Hansen, M. C., R. S. DeFries, J. R. G. Townshend, and?R. Sohlberg, 2000. Global land cover classification at 1km spatial resolution using a classification tree approach, *International Journal of Remote Sensing*, 21(6-7): 1331-1364.

Hansen, M. C., R. S. DeFries, J. R. G. Townshend, R. Sohlberg, C. Dimiceli, and M. Carroll, 2002. Towards an operational MODIS continuous field of percent tree cover algorithm: examples using AVHRR and MODIS data, *Remote Sensing of Environment*, 83(1-2): 303-319.

Huang, S., and F. Siegert, 2006. Land cover classification optimized to detect areas at risk of desertification in North China based on SPOT VEGETATION imagery, *Journal of Arid Environments*, 67(2): 308-327.

Inoue, Y., and A. Olioso, 2004. Synergistic linkage between remote sensing and biophysical models for estimating plant ecophysiological and ecosystem processes, *Journal of the Remote Sensing Society of Japan*, 24(1): 1-17.

Intergovernmental Panel on Climate Change (IPCC), 2007. Climate Change 2007, The Physical Science Basis, Contribution of Working Group I to the Fourth Assessment Report of the IPCC, Cambridge University Press, 996.

Irvin, B. J., S. J. Ventura, and B. K. Slater, 1997. Fuzzy and isodata classification of landform elements from digital terrain data in Pleasant Valley, *Wisconsin. Geoderma*, 77(2-4): 137-154.

Jang, J. D., 2006. Rural Land Cover Classification using Multispectral Image and LIDAR Data, *Korean Journal of Remote Sensing*, 22(2): 101-110.

Kalnay, E., M. Kanamitsu, R. Kistler, W. Collins, D. Deaven, L. Gandin, M. Iredell, S. Saha, G. White, J. Woollen, Y. Zhu, M. Chelliah, W. Ebisuzaki, W. Higgins, J. Janowiak, K. C. Mo, C. Ropelewski, J. Wang, A. Leetmaa, R. Reynolds, R. Jenne, and D. Joseph, 1996. The NCEP/NCAR 40-year reanalysis project, *Bulletin of the American Meteorological Society*, 77(3): 437-471.

Kim, D. H., S. G. Jeong, and C. H. Park, 2007. Comparison of Three Land Cover Classification Algorithms - ISODATA, SMA, and SOM - for the Monitoring of North Korea with MODIS Multi-temporal Data, *Korean Journal of Remote Sensing*, 23(3): 181-188.

Kimball, J. S., S. W. Running, and S. S. Saatchi, 1999. Sensitivity of boreal forest regional water flux and net primary production simulations to sub-grid-scale land cover complexity, *Journal of Geophysical Research-Atmospheres*, 104(D22): 27789-27801.

Kistler, R., E. Kalnay, W. Collins, S. Saha, G. White, J. Woollen, M. Chelliah, W. Ebisuzaki, M.

Kanamitsu, V. Kousky, H. van den Dool, R. Jenne, and M. Fiorino, 2001. The NCEP-NCAR 50-year reanalysis: Monthly means CD-ROM and documentation, *Bulletin of the American Meteorological Society*, 82(2): 247-267.

Koeppe, C. E., and G. C. De Long, 1958. *Weather and climate*, McGraw-Hill, 341.

Latifovic, R., and I. Olthof, 2004. Accuracy assessment using sub-pixel fractional error matrices of global land cover products derived from satellite data, *Remote Sensing of Environment*, 90(2): 153-165.

Lee, K. S., Y. S. Yoon, S. H. Kim, J. I. Shin, J. S. Yoon, and S. J. Kang, 2009. Analysis of Present Status for the Monitoring of Land Use and Land Cover in the Korean Peninsula, *Korean Journal of Remote Sensing*, 25(1): 71-83.

Liu, J., J. M. Chen, J. Cihlar, and W. Chen, 2002. Net primary productivity mapped for Canada at 1-km resolution, *Global Ecology & Biogeography*, 11(2): 115-129.

Lotsch, A., Y. Tian, M. A. Friedl, and R. B. Myneni, 2003. Land cover mapping in support of LAI and FPAR retrievals from EOS-MODIS and MISR: classification methods and sensitivities to errors, *International Journal of Remote Sensing*, 24(10): 1997-2016.

Loveland, T. R., J. W. Merchant, D. O. Ohlen, and J. F. Brown, 1991. Development of a land-cover characteristics database for the conterminous United States, *Photogrammetric Engineering and Remote Sensing*, 57(11): 1453-1463.

Melesse, A. M., and J. D. Jordan, 2002. A comparison of fuzzy vs. augmented-ISODATA classification algorithms for cloud-shadow discrimination from Landsat images, *Photogrammetric Engineering and Remote Sensing*, 68(9): 905-911.

Pasqualini, V., C. Pergent-Martini, G. Pergent, M. Agreil, G. Skoufas, L. Sourbes, and A. Tsirika, 2005. Use of SPOT 5 for mapping seagrasses: An application to Posidonia oceanica, *Remote Sensing of Environment*, 94(1): 39-45.

Park, Y. Y., K. S. Han, J. M. Yeom, and Y. C. Suh, 2006. An Adjustment for a Regional Incongruity in Global Land Cover Map: case of Korea, *Korean Journal of Remote Sensing*, 22(3): 1-11

Sandholt, I., J. Andersen, G. Dybkjaer, M. Lo, K. Rasmussen, J. C. Refsgaard, and K. H. Jensen, 1999. Use of remote sensing data in distributed hydrological models: applications in the Senegal River basin, *Danish Journal of Geography*, 99: 47-57.

Stibig, H. J., F. Achard, and S. Fritz, 2004. A new forest cover map of continental Southeast Asia derived from SPOT-VEGETATION satellite imagery, *Applied Vegetation Science*, 7(2): 153-162.

Stibig, H. J., A. S. Belward, P. S. Roy, U. Rosalina-Wasrin, S. Agrawal, P. K. Joshi, R. Beuchle, S. Fritz, S. Mubareka, and C. Giri, 2007. A land-cover map for South and Southeast Asia derived from SPOT-VEGETATION data, *Journal of Biogeography*, 34(4): 625-637.

Stone, T. A., P. Schlesinger, R. A. Houghton, and G. M. Woodwell, 1994. A map of the vegetation of South America based on satellite imagery, *Photogrammetric Engineering and Remote Sensing*, 60(5): 541-551.

Stroppiana, D., J. M. Grégoire, and J. M. C. Pereira, 2003. The use of SPOT VEGETATION data in a classification tree approach for burnt area mapping in Australian savanna, *International Journal of Remote Sensing*, 24(10): 2131-2151.

Tou, J. T., and R. C. Gonzalez, 1974. Isodata algorithm, Pattern Classification by Distance Functions, Pattern recognition principles,

Addison-Wesley, Reading, Massachusetts.

Townshend, J. R. G., C. O. Justice, and V. Kalb, 1987. Characterization and classification of South American land cover types using satellite data, *International Journal of Remote Sensing*, 8(8): 1189-1207.

Tucker, C. J., J. R. G. Townshend, and T. E. Goff, 1985. African land-cover classification using satellite data, *Science*, 227(4685): 369-375.

Vancutsem, C., J. F. Pekel, C. Evrard, F. Malaisse, and P. Defourny, 2009. Mapping and characterizing the vegetation types of the Democratic Republic of Congo using SPOT VEGETATION time series, *International Journal of Applied Earth Observation and Geoinformation*, 11(1): 62-76.

Verhoef, W., M. Menenti, and S. Azzali, 1996. Cover A colour composite of NOAA-AVHRR-NDVI based on time series analysis (1981-1992), *International Journal of Remote Sensing*, 17(2): 231-235.

Yang, D., and K. Musiake, 2003. A continental scale hydrological model using the distributed approach and its application to Asia, *Hydrological Processes*, 17(14): 2855-2869.